

Paleomagnetism, geochronology, and possible tectonic rotation of the middle Miocene Barstow Formation, Mojave Desert, southern California

BRUCE J. MACFADDEN *Florida Museum of Natural History, University of Florida, Gainesville, Florida 32611*

CARL C. SWISHER III *Berkeley Geochronology Center, 2453 Ridge Road, Berkeley, California 94709*

NEIL D. OPDYKE *Department of Geology, University of Florida, Gainesville, Florida 32611*

MICHAEL O. WOODBURNE *Department of Earth Sciences, University of California, Riverside, California 92521*

ABSTRACT

The Barstow Formation of the central Mojave Desert in the Mud Hills consists of 965 m of epiclastic and volcanic sediments deposited in an extensional rift. This widespread unit is of importance because its mammalian faunas characterize the Barstovian land-mammal age, previous isotopic ages on interbedded tuffs have been used to calibrate middle Miocene time, and it was deposited in a tectonically active region. Volcanic ash samples were collected from the Barstow Formation for isotopic dating using conventional ^{40}K - ^{40}Ar and $^{40}\text{Ar}/^{39}\text{Ar}$ single-crystal laser-fusion methods. Multiple analyses on minerals from 5 superposed tuffs yielded the following mean ^{40}K - ^{40}Ar ages: Rak Tuff at 16.3 ± 0.3 m.y., Oreodont Tuff at 15.9 ± 0.2 m.y., Dated Tuff at 14.8 ± 0.2 m.y., Hemicyon Tuff at 14.0 ± 0.1 m.y., and Lapilli Tuff at 13.4 ± 0.2 m.y. Similar mean ages were also obtained on the following tuffs using single-crystal $^{40}\text{Ar}/^{39}\text{Ar}$ laser-fusion methods: Oreodont Tuff at 15.9 ± 0.06 m.y., Dated Tuff at 14.8 ± 0.06 m.y., and Hemicyon Tuff at 14.0 ± 0.09 m.y.

In order to develop a local magnetostratigraphy, 272 paleomagnetic sites were collected from 7 important sections within the Mud Hills. Saturation isothermal-remnance experiments suggested the presence of either hematite or magnetite as carriers of remanence. After either stepwise alternating-field or thermal demagnetization, characteristic directions were usually isolated between 30 and 50 mT or 300 and 500 °C. Positive reversal and fold tests indicate a stable remanence acquired prior to folding. There are 21 magnetic polarity zones interpreted from the continuous part of the Barstow Formation in the study area. By using the 5 isotopic ages determined from interbedded tuffs, the local composite polarity pattern is correlated to the top of chron C5D through the bottom of C5AB on the magnetic polarity time scale, or an age range from 17.6 to 13.4 m.y. The boundary between Hemingfordian and Barstovian land-mammal ages herein occurs 30 m below the Oreodont Tuff (15.8 ± 0.2 m.y.) within C5B and is taken at about 16.0 m.y. ago. The Barstow formational mean declination is 347.1° ($\text{inc} = 47.5^\circ$, $\alpha_{95} = 6.51^\circ$; $\Delta D = 7.97^\circ$), suggesting negligible or possibly slight counterclockwise rotation ($R = 4.1^\circ$; $\Delta R = 10.5^\circ$) for this part of the Mojave block during the past 18 m.y. A $^{40}\text{Ar}/^{39}\text{Ar}$ mean age of 19.3 ± 0.02 m.y. for the Red Tuff, which is near the local base of the Barstow Formation and unconformably underlying our composite section, constrains a minimum age for the beginning of local basin filling with principally epiclastic sediments.

INTRODUCTION

The fossiliferous upper Tertiary deposits of the Mojave Desert have been of great interest to vertebrate paleontologists because the Barstovian land-mammal age takes its name from the stage of faunal evolution represented in the Barstow Formation in this region (Wood and others, 1941; Tedford and others, 1987; also see Woodburne and others, 1990). More recently, with increased interest in the tectonics of the San Andreas fault system and adjacent areas of southern California, the Mojave Desert has received much attention with regard to structural models and paleomagnetic data explaining the geologic development of this region (for example, Garfunkel, 1974; Luyendyk and others, 1980; Dokka, 1983, 1986, 1988; Hornafius and others, 1986; Luyendyk and Hornafius, 1987; Ross and others, 1987, 1988, 1989).

The Barstow Formation has figured prominently in the calibration of middle Miocene land-mammal evolution in North America. The isotopic dating of this unit in the Mud Hills was first addressed by Evernden and others (1964) in their classic calibration of Cenozoic mammalian chronology of North America. They published ^{40}K - ^{40}Ar dates from two tuffaceous horizons in the Barstow Formation in the Mojave Desert. Of these, the "Dated Tuff" in the Rainbow basin was the first numerical calibration point for Barstovian fossils from the Mud Hills. (The other, from the Cronese basin, is located some 60 km to the northeast; see Woodburne and others, 1990.) Their age for the "Dated Tuff" was 15.5 m.y. (corrected for new decay constants; Dalrymple, 1979), although no error limits were given.

Savage and Curtis (in Lindsay, 1972) later added an additional ^{40}K - ^{40}Ar calibration point, the "Lapilli Sandstone," located in the upper part of the Barstow Formation in the Mud Hills. The analyses yielded ages (corrected) of 13.6 m.y. on biotite and 13.8 m.y. on plagioclase. Woodburne and Tedford (1982) and Woodburne and others (1982) also published additional ^{40}K - ^{40}Ar dates on biotite-bearing tuffs from the Barstow Formation. The stratigraphically lowest date (Woodburne and others, 1982) of 16.3 ± 0.3 Ma comes from the Oreodont Tuff; the intermediate date of 14.8 ± 0.3 Ma comes from the Dated Tuff; and the upper date of 13.3 ± 0.7 Ma comes from the Hemicyon Tuff (see below for exact stratigraphic position).

Burke and others (1982) added two dates for the Barstow Formation. Although the sample localities are not in direct association with the fossil vertebrate localities in the Mud Hills, the ages add important information on the regional duration of the Barstow Formation. An age of 13.5 ± 0.2 m.y. was reported on the Andesite of Murphy's Well, which is thought to correlate with the uppermost part of the Barstow Formation. A basalt

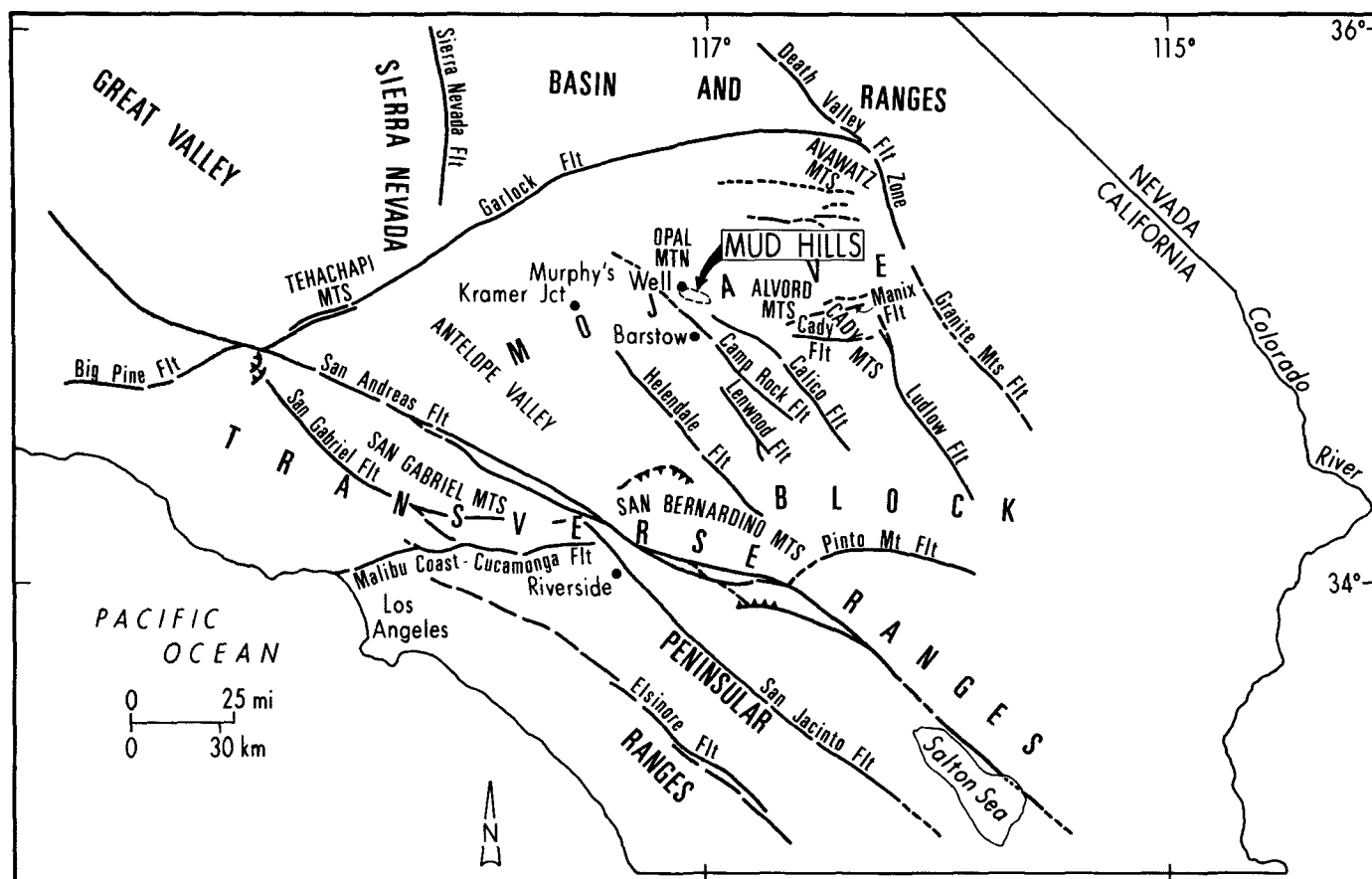


Figure 1. Geographic and geologic setting of the Mojave Desert relative to major structural features in southern California. After Geologic Map of California; Bakersfield, Trona, Kingman, Los Angeles, San Bernardino, Needles, Long Beach, Santa Ana, Salton Sea sheets.

from near the local base of the Barstow Formation yielded a whole-rock ^{40}K - ^{40}Ar date of 16.5 ± 0.4 Ma.

Despite these available isotopic determinations, the precise age of the Barstow Formation, and hence middle Miocene land-mammal evolution, has not been calibrated by the most modern geochronological techniques currently available. Therefore, the purpose of this paper is to present results of a detailed paleomagnetic and geochronological analysis of this formation as it is exposed in the Mud Hills (also known as the Barstow syncline) located about 15 km north of the city of Barstow, California. The emphasis in this report will be on the magnetic polarity stratigraphy, new isotopic dates, and new paleomagnetic data bearing on previous hypotheses of tectonic rotations in this region. The detailed lithostratigraphic descriptions and mammalian biochronology of the Barstow Formation as well as relevant isotopic dates from localities outside the Mud Hills are presented in Woodburne and others (1990).

GEOLOGIC SETTING

The Barstow Formation crops out extensively in the Mojave Desert, a region located at about lat. 35°N and long. 117°W (Fig. 1). The Mojave Desert is also a structural entity, usually termed the "Mojave block," as used below (for example, Garfunkel, 1974; Dokka, 1986), or the "Mojave rift" (Dokka, 1988). Roughly rhomboidal, it is bounded on the southwest by the San Andreas fault zone and the Transverse Ranges, on the north by the Garlock fault zone, and to the east by the Death Valley and Granite Mountain faults. First-motion seismic and other geologic studies indicate

that many of these faults are still active today (Garfunkel, 1974). Because the region is close to a major plate boundary and near the San Andreas fault system, the late Cenozoic geologic evolution is exceedingly complex, as is discussed below.

The approximately 1,000 m of epiclastic and volcanoclastic sediments of the Barstow Formation was deposited during the middle Miocene in an east-west-trending elongate basin (Fig. 1) within the central Mojave block (Dokka, 1986; see Woodburne and others, 1990, for a detailed lithostratigraphic description). This basin was subsequently folded into structures that generally trend east-west and are cut by faults that trend $\text{N}50^\circ\text{W}$. These faults, thus younger than the Barstow Formation, are otherwise constrained as being in part younger than the Black Mountain Basalt, dated at 2.55 ± 0.58 Ma (Burke and others, 1982), which locally overlies them to the west of the Mud Hills. Some of these right-lateral faults have been active during the Holocene (for example, Garfunkel, 1974; Carter and others, 1987). The Mojave block also is cut by a small number of east-west-trending faults, for which left-lateral separation is generally inferred. Some of these, for example, the Manix fault, also have been active during the Holocene (Garfunkel, 1974). During the early Miocene and prior to the deposition of the Barstow Formation, the Mojave block apparently experienced a major episode of detachment faulting, uplift, and extensional rifting (Dokka, 1986).

Models of regional lithospheric plate interaction for western North America (Atwater, 1970) suggest that as the North American plate overrode the adjacent subduction zone and spreading center of the Pacific plate at about 30 Ma, the strain between the two plates was partially relieved by

the then-developing San Andreas fault. Although it is difficult to develop unequivocal evidence for the beginning of slip on the San Andreas fault in southern California, the volcanism, extension, uplift, and rifting within the Mojave block that took place from about 26 to 18 Ma (Dokka, 1986; Dokka and Woodburne, 1986) probably reflects the beginning of the tectonic regime related to the San Andreas fault.

FIELD AND LABORATORY METHODS

Paleomagnetic Analyses

In the field, a minimum of 3 separately oriented paleomagnetic hand samples were collected from 272 sites located throughout the Barstow

Formation in the Mud Hills. The average vertical separation between sites was 8 m except where no suitable lithologies were available; that is, they were either too coarse or too poorly consolidated (or both). In addition, several important marker horizons (for example, the Skyline Tuff) were intensively sampled at denser intervals vertically and horizontally to establish their paleomagnetic signatures for lithostratigraphic correlations.

Paleomagnetic samples were collected from seven measured sections within the Barstow syncline; three from the south limb and four from the north limb (also see Fig. 7, below). All sites were precisely located on our measured sections and aerial photographs. The seven sections were selected because each was relatively continuous, represented either limb of the syncline (for a paleomagnetic fold test), or contained existing or potential isotopic control or important fossil-mammal localities (for example,

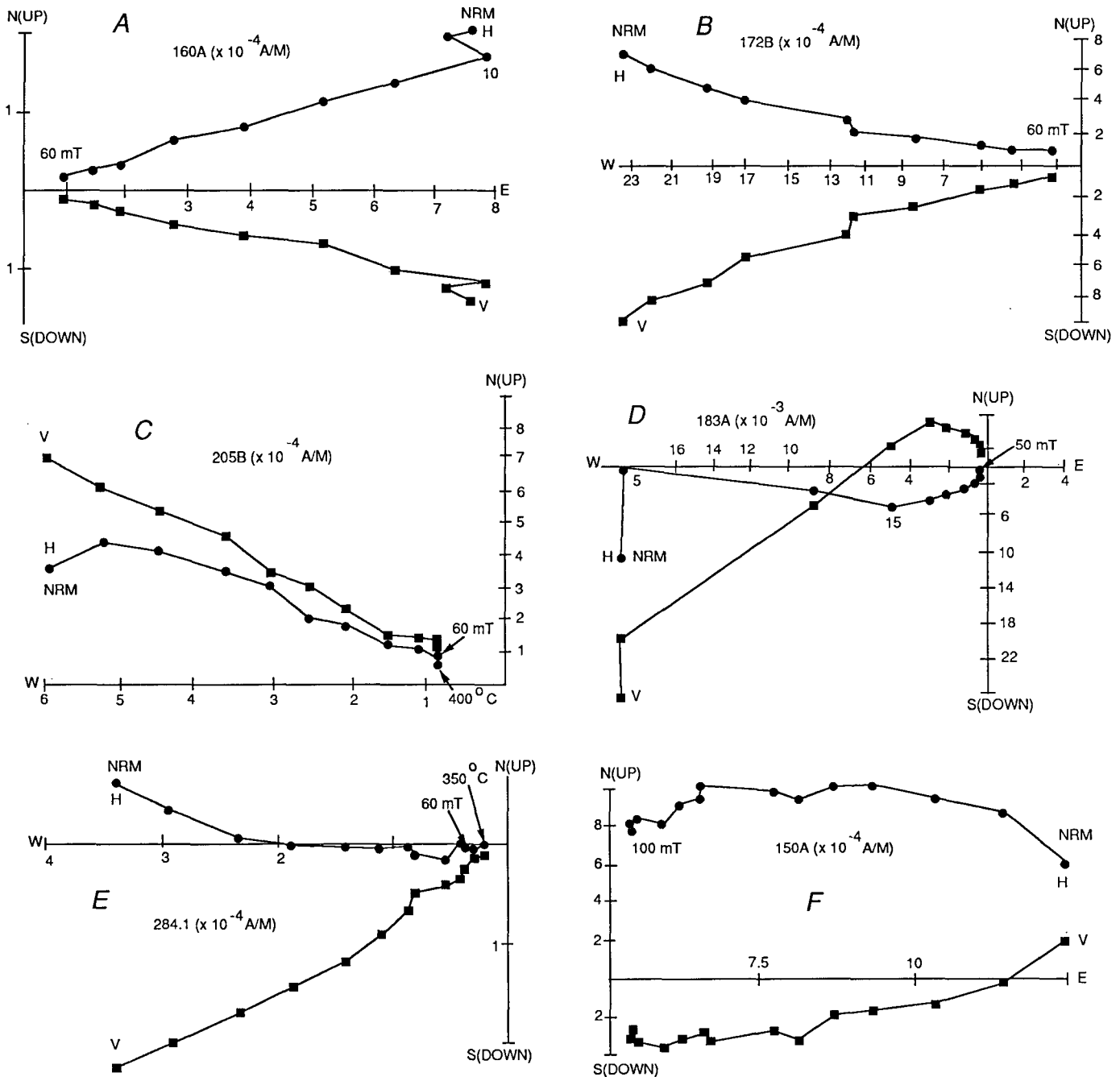


Figure 2. Orthogonal vector diagrams showing decay characteristics after alternating-field demagnetization for selected samples from the Barstow Formation.

Lindsay, 1972). Taken together, these form a composite section that spans the known thickness of the Barstow Formation in this region.

In the laboratory at the University of Florida, the paleomagnetic samples were prepared into 2.54-cm cubes, measured using a SCT two-axis cryogenic magnetometer (Fuller and others, 1985), and progressively demagnetized with either Schonstedt alternating-field (AF) or thermal demagnetizers. The Barstow Formation contains a variety of epiclastic lithologies. Accordingly, about 10% of the sites, chosen from the spectrum of lithologies, were chosen for pilot blanket demagnetization studies to better understand the magnetic characteristics of the Barstow sediments. For each of these sites, the first sample was subjected to AF demagnetization in 8 to 11 steps at fields between 5 and 50 mT; the other was subjected to thermal demagnetization in 10 to 12 steps between 100 and 640 °C. Although some sites demagnetized well using AF (Figs. 2A and 2B),

others did not (Figs. 2C and 2F) owing to high-coercivity components of magnetization. Despite the lack of a stable vector decay toward the origin, in some samples (for example, 2F) the polarity could be inferred from the position of the horizontal and vertical components. In general, thermal demagnetization (Fig. 3) seemed to characterize the stable remanence in more samples better than did AF demagnetization. Also, it was impossible to determine, *a priori*, when AF demagnetization might result in unrecovered high-coercivity components. Therefore, the remaining samples from all other sites were thermally demagnetized (in 2 to 10 steps) between 400 and 550 °C and in certain cases, as high as 660 °C. The majority of sites responded better to thermal demagnetization (Fig. 3), but in some cases, AF resulted in a more linear, stable decay to the origin, as indicated by the vector demagnetization diagrams (Fig. 2). In order to insure that the normally magnetized sites (with positive inclinations) were

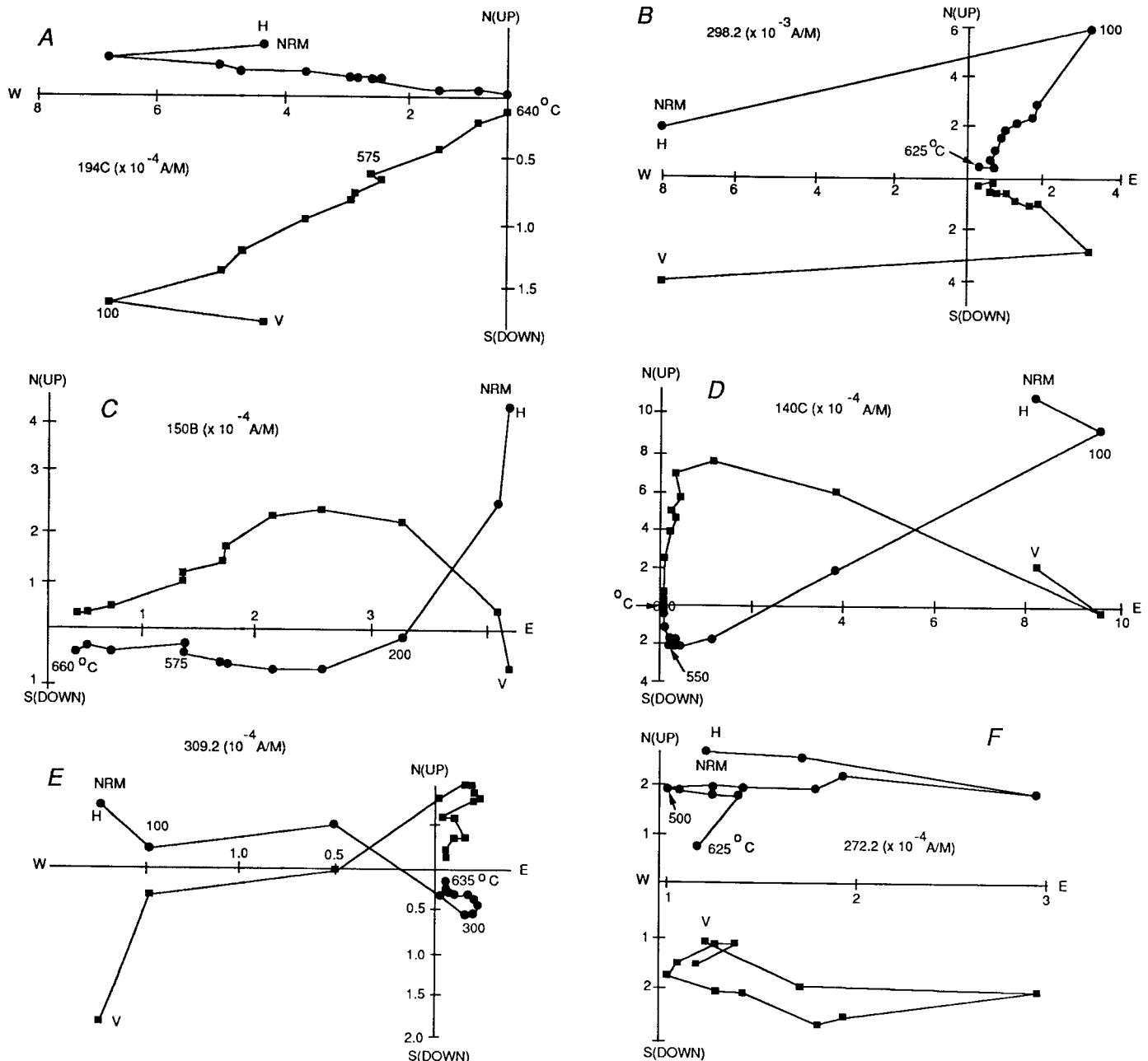


Figure 3. Orthogonal vector diagrams showing decay characteristics after thermal demagnetization for selected samples from the Barstow Formation.

not overprinted, samples originally subjected to AF demagnetization were subsequently treated by thermal demagnetization between 300 and 500 °C. If this combined regime of AF and thermal demagnetization was used, unambiguous polarities could be determined for the majority (63%) of sites; however, for the remaining 37%, polarities were still indeterminate (see statistical analysis below).

In general, there was little systematic pattern of demagnetization characteristics related to gross lithology. The most apparent pattern was that the reddish-brown, hematite-bearing (as demonstrated by saturation isothermal remanence studies), coarse sediments in the lower third of the Barstow Formation (Lower Member) responded better to thermal demagnetization. In the upper two-thirds of the formation, which consists of apparently less oxidized sediments, there was no *a priori* indication of predicted demagnetization characteristics. In order to better understand the origin of the magnetization of the Barstow section, pilot saturation isothermal remanence studies were done on 10 sites representing different lithologies. In samples from the Lower Member (Figs. 4A and 4B), saturation does not occur in fields of as much as 800 mT, indicating that hematite is the predominant magnetic mineral. In the middle and upper parts of the section, the samples (Figs. 4C–4F) become saturated between 150 and 200 mT, indicating that the predominant magnetic mineral is magnetite or titanomagnetite. The mean NRM intensity of all samples measured is 2.27×10^{-3} A/m ($N = 730$). After demagnetization, intensities averaged, for example, 0.8 ± 10^{-3} A/m for 40 mT ($N = 90$) and 0.6×10^{-3} A/m for 400 °C ($N = 620$). For all samples demagnetized at three or more steps, principal component analysis (Kirschvink, 1980) was done to determine least-squares best fit of the characteristic component of magnetization as determined from linear decay toward the origin on orthogonal vector diagrams (for example, Fig. 2). For sites in which some samples had

a direction determined by the principal component method and other sample directions that were interpreted from a single step, these data were then combined to determine Fisher mean directions (Fisher, 1953).

Isotopic Age Analyses

Sample Collection. Samples of the ashes to be dated were collected in stratigraphic context with the paleomagnetic transects where unambiguous superpositional relationships with associated fossil-bearing strata were carefully documented. The sampled units were chosen as a result of their relative stratigraphic position, their proximity to fossil localities, and their overall suitability for isotopic dating. Every attempt was made to collect the freshest, least weathered rock samples. The factors considered include: (1) grain size of K-bearing minerals; (2) absence of older, re-worked igneous or volcanic detrital grains; and (3) minimal amount of visible weathering or alteration of K-bearing minerals. Some samples, such as the Rak Tuff, did not meet all of these criteria; however, no other samples were found in this part of the Barstow Formation. Samples such as the Rak Tuff may still be dated, but must be interpreted with great caution because they commonly yield less reliable data and/or they require considerably more extensive analysis to identify alteration and/or identification of age components from multiple volcanic events.

Mineral Separations. At the Berkeley Geochronology Center (BGC), rock samples were examined using binocular and petrographic microscopes to identify the freshest datable minerals and to further identify the presence of possible alteration and/or contamination. The samples were crushed and sieved according to the size of the contained minerals. Bulk mineral separations follow standard magnetic and density mineral-separation techniques. All feldspars were treated with HF in an ultrasonic bath to remove any composite glass and then were boiled in distilled water to reduce surficial atmospheric Ar. Biotites and hornblendes were treated only with distilled water in an ultrasonic bath to remove attached devitrified glass, to loosen composite grains, and to reduce surficial atmospheric Ar.

For the preparation of $^{40}\text{Ar}/^{39}\text{Ar}$ analyses, a small bulk sample was crushed, washed in distilled water, and sized according to its K-bearing minerals. Samples were bathed in distilled water to remove composite grains and attached devitrified glass. Feldspars were treated with HF as in the bulk samples. Euhedral minerals to be dated were hand-picked from samples, using a binocular microscope.

Isotopic Analyses. For ^{40}K - ^{40}Ar age determinations, K analyses were made on sample splits of mineral separates in duplicate using a Zeiss PF-5 flame photometer following procedures described by Carmichael and others (1968). Variation in K content between duplicate analyses is reflected in the 1σ confidence figure calculated for the age. Ar isotopic abundances of gas extracted after total fusion of sample splits were measured on Reynolds-type noble-gas mass spectrometers using isotope dilution by calibrated ^{38}Ar spikes, metered to a pipette system.

Completion of a new extraction line coupled with a Mass Analysis Product "MAP 215" extended geometry mass spectrometer recently became operational at the BGC. This now allows $^{40}\text{Ar}/^{39}\text{Ar}$ analyses using the single-crystal laser-fusion technique. The enhanced sensitivity of the MAP spectrometer allows the accurate measurement of much smaller amounts of Ar gas than was previously possible using the Reynolds-type mass spectrometers. The BGC employs standard $^{40}\text{Ar}/^{39}\text{Ar}$ dating techniques (Dalrymple and Lanphere, 1968) in which isolated crystals of biotite or feldspar are fused using a coherent Innova 90 Series Ion Laser.

Age Reduction. The calibration and depletion rates of the ^{38}Ar spike were established by control dates on in-house, highly radiogenic biotite standards JFE64-29 and GHC305 and are in turn calibrated with inter-

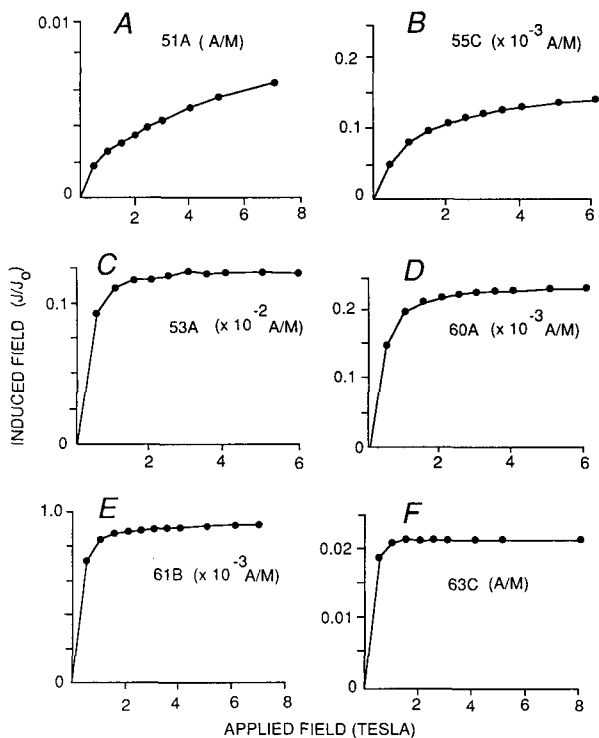


Figure 4. Plots of saturation isothermal remanence (IRM) versus applied field for six representative samples from the Barstow Formation.

laboratory standards of known age and by first principles using gas laws, atmospheric abundance and isotopic composition, and the assumption of invariant volumes in the precisely manufactured air pipettes. The decay constants used in the age calculations are those recommended by Steiger and Jaeger (1977), that is, $\lambda_{\epsilon} + \lambda_{\epsilon'} = 0.581 \times 10^{-10} \text{ yr}^{-1}$; $\lambda_{\beta} = 4.962 \times 10^{-10} \text{ yr}^{-1}$; $^{40}\text{K}/\text{K}_{\text{Total}} = 1.167 \times 10^{-4}$.

All $^{40}\text{Ar}/^{39}\text{Ar}$ samples were irradiated in the University of California TRIGA reactor for 10 hr (except the 86CS-BCC1 sanidine, which was irradiated for 1 hr). Isolated crystals of biotite and feldspar were fused using a Coherent Innova 90 Series Ion Laser. The extraction system is on-line with the MAP 215 mass spectrometer. Procedures are comparable to those in Dalrymple and others (1981). J values were calculated using multiple standards, primarily based on the well-known ages of P207, MMHb, and GHC305. The following K and Ca corrections were determined using optical grade CaF_2 and a laboratory potassium glass: $^{40}\text{Ar}_{\text{K}}/^{39}\text{Ar}_{\text{K}} = 0.002$, $^{39}\text{Ar}_{\text{Ca}}/^{37}\text{Ar}_{\text{Ca}} = 0.000730$, and $^{36}\text{Ar}_{\text{Ca}}/^{37}\text{Ar}_{\text{Ca}} = 0.000277$.

At the BGC, error estimates that accompany each ^{40}K - ^{40}Ar age analysis routinely represent 1σ (standard deviation). The 1σ error bar that accompanies each ^{40}K - ^{40}Ar age analysis reflects estimates of precision based on how well that particular gas was measured. These errors incorporate variation calculated in the measurement of (1) duplicate K analyses by flame photometry, (2) nonradiogenic $^{40}\text{Ar}/^{38}\text{Ar}$ ratio determined from zero-age curve, (3) $^{36}\text{Ar}/^{38}\text{Ar}$ spike composition, (4) $^{40}\text{Ar}/^{38}\text{Ar}$ and $^{38}\text{Ar}/^{36}\text{Ar}$ initial ratios of gas at time of entry into the spectrometer, and (5) moles of ^{38}Ar in spike calibrated from known age samples. The contribution of each component error to the total uncertainty in age is calculated by a propagation-of-errors formula (A. Deino and R. H. Drake, unpub. data). Analytical accuracy of a single age determination is based on the calibration of the ^{38}Ar spike.

Mean ages of multiple ^{40}K - ^{40}Ar and $^{40}\text{Ar}/^{39}\text{Ar}$ analyses report both 1σ and standard error of the mean (SEM). Reproducibility, including variation in K content of GHC305 during the present study, was less than 0.5% (1σ) and 0.1% (SEM) on 12 Ar and 6 K analyses. Although the reported precision of some multiple analyses may be better than these errors, our accuracy is limited to approximately 0.5% (1σ) and 0.1% (SEM). We report the calculated precision, however, as it is useful when comparing ages of other dated units using the same calibration parameters.

PALEOMAGNETIC RESULTS

All site data were analyzed using Fisher statistics (Fisher, 1953). If the significance point (R) criteria summarized in Irving (1964, Table 4.4) are used, sites for which the data were random can be rejected from formational mean calculations. After combining sites at the same horizons

(from different sections or lateral locations) and the filtering described above, 134 sites were statistically significant. Of these, 125 were interpreted to represent either normal or reversed polarity; that is, intermediate directions were dropped from further analysis (Table 1). The overall formational mean (reversed sites inverted) is dec. 347.11° , inc. $47.50^\circ \pm 5.38^\circ$ (α_{95} , see Table 1, entry 1). As represented in Figure 5, relative to the NRM directions, the demagnetization regime described above seems to adequately isolate two antipodal populations, one in the northern hemisphere with positive inclinations and the other in the southern hemisphere with negative inclinations interpreted to represent, respectively, normal and reversed polarities.

Stability Tests

Reversal Test. The combined mean directions of two groups, that is, the statistically significant normal and reversed (Table 1, entries 3 and 4) sites, are plotted in Figure 6. With respect to the α_{95} , there is no difference between the directions of the two data sets, suggesting that the Barstow sediments retain a stable characteristic magnetization and that significant secondary overprints were satisfactorily removed by demagnetization.

Fold Test. By using the *F*-test (McElhinny, 1964), the ratio of precision parameters (k_2/k_1) was compared for the tilt-corrected and *in situ* formational mean directions. The *F*-value of 1.37 (Table 1, entries 1 and 2) is greater than that expected (1.32) at $p = 0.05$ for $N = 125$ (*F*-value taken from Rohlfs and Sokal, 1969). Therefore, the null hypothesis of no difference is rejected for the tilt and geographic (*in situ*) data sets, which indicates a positive fold test. McFadden and Jones (1981) proposed a more elaborate fold test; however, their conclusions indicate that if a data set passes a positive fold test using the *F*-value (McElhinny, 1964), then assuming similar precision parameters from different limbs of the structure in question, both tests will have the same conclusion.

In summary, given the demagnetization characteristics (linear decay segments represented in Figs. 2 and 3), distribution of Fisher mean Class I data (Fig. 5C), and positive reversal (Fig. 6) and fold tests, it is concluded that the magnetizations are stable and were acquired during the Miocene before folding of the Barstow Formation.

Interpretation of Site Polarities

As a result of the laboratory and statistical analyses, 170 of the 272 original sites yielded data from which interpretations of polarity could be made. The 170 sites fell into the following designations of Opdyke and others (1977): Class I, 125 sites (3 or more statistically significant, concordant directions from 3 or more samples); Class II, 4 sites (only 2 samples available yielding concordant directions); Class III, 41 sites (3 or more

TABLE 1. FISHER PARAMETERS FOR STATISTICALLY SIGNIFICANT PALEOMAGNETIC SITES FROM THE BARSTOW FORMATION

Data set	Dec.	Inc.	N	R	α_{95}	K	ΔD^*
1. All sites (R inverted), tilt corrected	347.11	47.50	125	106	5.38	6.51	7.97
2. All sites (R inverted), <i>in situ</i> coordinates	352.56	55.80	125	99	6.50	4.76	
3. All N sites, tilt corrected	352.78	46.42	69	59.7	6.79	7.32	9.87
4. All R sites, tilt corrected	159.55	-48.45	56	46.6	8.64	5.83	13.08
5. All sites (R inverted), S limb, tilt corrected	345.95	48.94	71	58.3	7.90	5.53	
6. All sites (R inverted), N limb, tilt corrected	348.46	45.72	54	47.7	7.14	8.35	
7. All sites (R inverted), S limb, <i>in situ</i> coordinates	333.12	68.76	71	59.4	7.48	6.05	
8. All sites (R inverted), N limb, <i>in situ</i> coordinates	4.02	36.29	54	44.7	8.92	5.71	

* ΔD is error estimation of Demarest (1983).

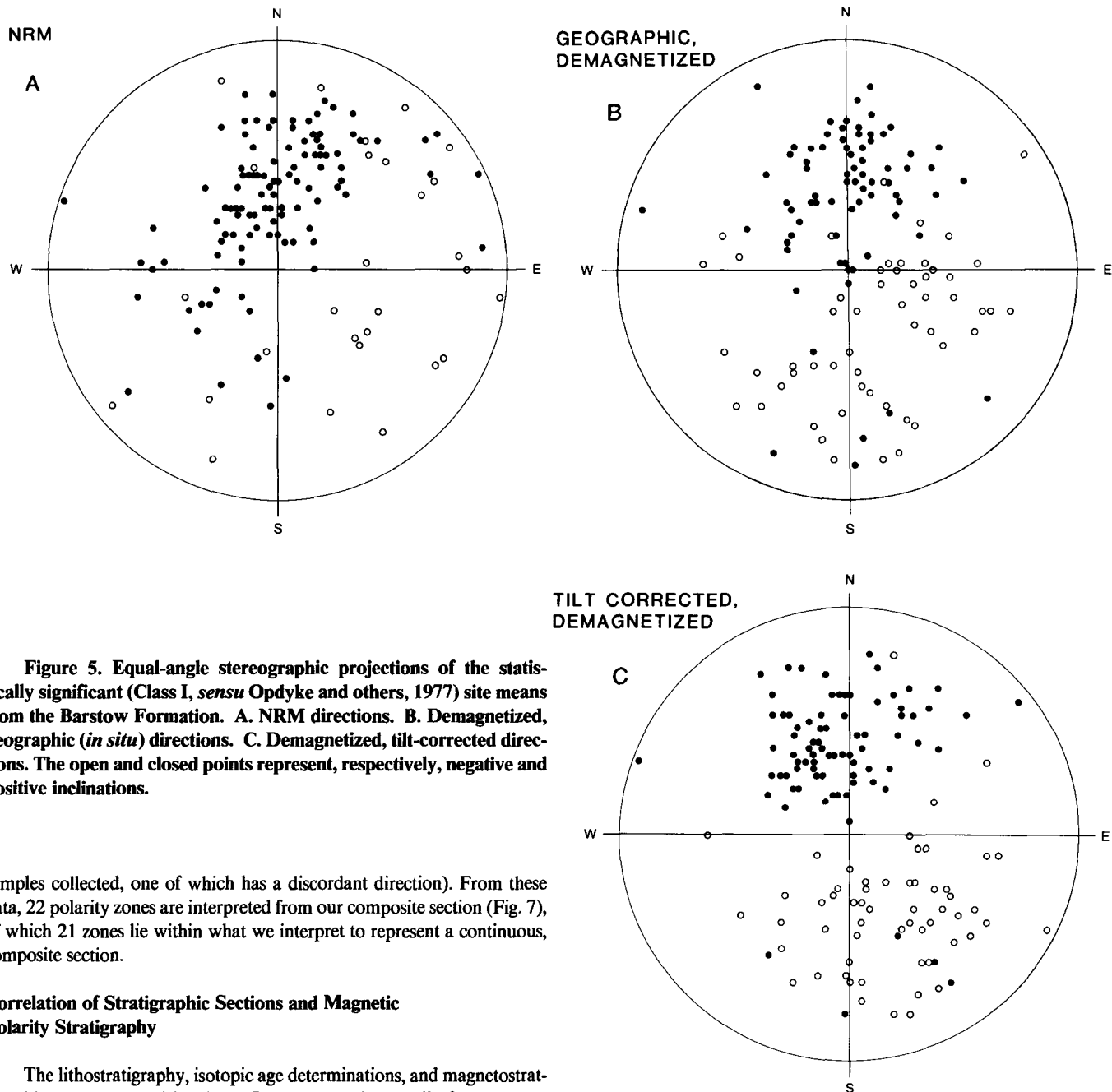


Figure 5. Equal-angle stereographic projections of the statistically significant (Class I, *sensu* Opdyke and others, 1977) site means from the Barstow Formation. A. NRM directions. B. Demagnetized, geographic (*in situ*) directions. C. Demagnetized, tilt-corrected directions. The open and closed points represent, respectively, negative and positive inclinations.

samples collected, one of which has a discordant direction). From these data, 22 polarity zones are interpreted from our composite section (Fig. 7), of which 21 zones lie within what we interpret to represent a continuous, composite section.

Correlation of Stratigraphic Sections and Magnetic Polarity Stratigraphy

The lithostratigraphy, isotopic age determinations, and magnetostratigraphic data presented in Figure 7 are arranged generally from west to east. The first-order correlation of the individual sections was determined by the use of prominent marker horizons, namely the Oreodont Tuff at 474 m, Skyline Tuff at 774 m, Hemicyon Tuff at 838 m, and the Lapilli Sandstone at 960 m, as well as the distinctive lithologies represented by the members of the Barstow Formation. The detailed correlations among the sections that we use to assemble a composite sequence are as follows.

Section 1. Rainbow Loop–South Limb. This is the longest of our measured sections and is exposed south and west of Rainbow basin (Fig. 7); it contains 19 magnetozones (R1–R10). R1 and the lower part of N1 lie unconformably below the remainder of the section, the latter of which is interpreted to be continuous. The normal sites above and below the unconformity are both termed “N1,” although these could also represent different events on the magnetic polarity time scale (MPTS). The Rak Tuff (16.3 ± 0.3 Ma) occurs near the base of magnetozone N2; the Oreodont

Tuff (15.8 ± 0.2 Ma) lies near the middle of zone R6; the Skyline Tuff occurs near the base of magnetozone N9. The tuffaceous beds and units composed of fine-grained sandstone, claystone, and mudstone are clearly of lacustrine origin and represent relatively slow rates of accumulation. Intervals in section 1 composed of such units are found principally between the Rak and Oreodont Tuffs, and from just below the Skyline Tuff to the top of the local section. Intervals that are composed largely of conspicuously coarse-grained deposits are prominently developed from the base of the section to the Rak Tuff, and from slightly above the Oreodont Tuff to just below the Skyline Tuff. Clasts in the conglomeratic units within magnetozones R6 to R9 are commonly very angular and most likely alluvial rather than fluvial in origin. It is likely that these coarse-grained units reflect nearby tectonic adjustments in the location of the

basin margin. Other evidence of such adjustments is the observation that the Rak Tuff rises in its relative stratigraphic position about 30 m within 100 m eastward of the main traverse of section 1.

Section 2. Carnivore Canyon–North Limb. The Oreodont, Skyline, and Hemicyon Tuffs have been identified in section 2, with the Oreodont and Skyline Tuffs demonstrating unequivocal correlation to section 1 on the south limb of the Barstow syncline. There is 67 m of section between the Oreodont and Skyline Tuffs in Carnivore Canyon versus about 300 m between these units in section 1. Both sections were carefully examined in the field for evidence of faulting that would either add or subtract section in these two sequences. None was found, indicating that the great attenuation of section in Carnivore Canyon is probably due to lower rates of sediment accumulation.

Paleomagnetic data suggest that the Skyline Tuff in both sections 1 and 2 represents magnetozones N9. With regard to the Oreodont Tuff, if rates of sedimentation are adjusted, then the fivefold difference in Carnivore Canyon relative to Rainbow Loop suggests that the reversed-polarity interval that brackets the Oreodont Tuff in Carnivore Canyon corresponds to the interval represented by R6 through R8, inclusive, in the Rainbow Loop section, and the short magnetozones N6 and N7 in the Rainbow Loop section apparently were too brief to be recorded in the Carnivore Canyon section, or they occurred during undetected hiatuses.

The normal-polarity zone immediately below the Skyline Tuff in Carnivore Canyon appears to represent magnetozones N8 in the Rainbow Loop section. The interval between the Oreodont and Skyline Tuffs is much thicker on the southeastern side of the basin as compared to that on the northwestern side. Presumably, the basin margin was nearer to the southeast, and the more central part was located to the northwest.

In Carnivore Canyon (section 2), the succession above the Skyline Tuff records a reversal at the level correlative with the Dated Tuff (R10) in section 1, followed upward by mostly normal polarity. This normal zone probably represents N10 in our composite section, although the exact correlation is uncertain because the middle of section 2 contains a fault.

Hell Gate and Hemicyon Quarry Basins—Sections 6 and 7. Both sections show a unit, the Hemicyon Stratum, that is followed upward by a biotitic tuff (locally a biotitic sandstone). This tuff, known as the “Hemicyon Tuff,” has been dated in sections 2 and 7 at ca. 14.0 Ma. An unusually thick sequence of limestone beds occurs below this tuff in section 2, the base of which is here interpreted to be the Hemicyon Stratum (section 7; Fig. 7).

Above the Hemicyon Tuff at Hemicyon Quarry basin, a succession of brown-gray to green- or yellowish-gray siltstone beds and thin calcareous tuffs is capped by another white biotitic tuff. An equivalent interval in Hell Gate basin is composed of a succession of mainly cherty limestones and siltstones, with some of the limestones apparently having been tuffaceous. At Hell Gate basin, these sediments are capped by a thick (~0.3 m) white biotitic tuff that is a prominent marker bed in this sequence. In both sections 6 and 7, a thick sequence of hornblende-rich sandstones, tuffs, and an upper lapilli tuff (the Lapilli Sandstone) are found. This is capped by a thick (~6 m) sequence of limestone beds. Except for slight sedimentary and thickness differences due to facies, the succession from the Hemicyon Stratum through the Lapilli Sandstone is essentially identical in both the Hemicyon Quarry and Hell Gate basins. Beds traced westward from Hell Gate basin, toward Carnivore Canyon, clearly show a pinchout of the hornblende-bearing sandstones and associated Lapilli Sandstone, together with a thickening of orange-red conglomerate beds with granitic detritus that occupy a position below the Lapilli Sandstone and above the subjacent thick biotitic tuff of Hell Gate basin. The coarse-grained granitic conglomerate and sandstone beds increase in number westward until, at Carnivore Canyon, they represent about 50% of the deposits above the

biotitic tuff dated at 14.0 Ma. This tuff constitutes a sequence of tuffs and tuffaceous sandstones about 5 m thick at Carnivore Canyon. The stratigraphic equivalent of the thick tuff at Hell Gate basin (just below the hornblende-rich sandstone and tuff sequence) has not been identified in Carnivore Canyon, where it presumably has been masked or removed by a paleo-stream that carried coarse-grained granitic alluvial gravels apparently deposited at the local basin margin.

Thus, as shown in Figure 7, the upper half of the thick magnetozones N10 in Carnivore Canyon consists of thick arkosic sandstone and conglomeratic beds. These apparently form a wedge that with interbedded finer-grained siltstone and claystone units, thins eastward to within 0.25 km of Hell Gate basin and feathers out to a single bed that occurs stratigraphically just below the hornblende-rich interval and above the thick biotitic tuff. This conglomeratic sandstone is not present in the Hell Gate basin succession 0.25 km to the east, but the comparable interval should be represented by deposits just above (~1 m) the thick biotitic tuff at that locality. Although the thick biotitic tuff of the Hell Gate basin is not recognized in the top of the Carnivore Canyon section, these two sections are correlated by the presence in both of magnetozones R11.

If these interpretations are correct, then the Lapilli Sandstone at Hell Gate basin (which lies in a normal magnetozones N11) is stratigraphically higher and chronologically younger than the measured top of the Carnivore Canyon section and represents the youngest deposits of the Barstow Formation (including the capping limestone) on the north limb of the Barstow syncline. This section appears to be coeval with the lithologically comparable hornblende-rich sandstone, Lapilli Tuff, and capping limestone at the Hemicyon Quarry basin (section 7; Fig. 7) on the south limb of the syncline and also correlates lithostratigraphically with the top of the Barstow Formation exposed at Rodent Hill basin (section 3, Fig. 7), which also has a reversed magnetozones, identified herein as R11. Note that our section on the north limb of the syncline in Rodent Hill basin does not include the stratigraphically lower intervals as presented by Lindsay (1972, Pl. 1).

Johnson and McGee (1983) calculated the probability of capturing all reversals in a particular stratigraphic section, given (1) a uniform sampling regime, (2) the number of sites collected (N), and (3) reversals encountered (R). When the calculated sampling probability, $p = R/(N - 1)$, is < 1 , then the geometry of a given sampling program is sufficient to find the major reversals (that is, those with a duration of 10^5 yr or more) that are recognized on the MPTS. For the Barstow Formation, $p = 0.07$, suggesting that our sampling density and interpreted magnetostratigraphy are sufficiently detailed to correlate to the time scale if there are no major sedimentological hiatuses.

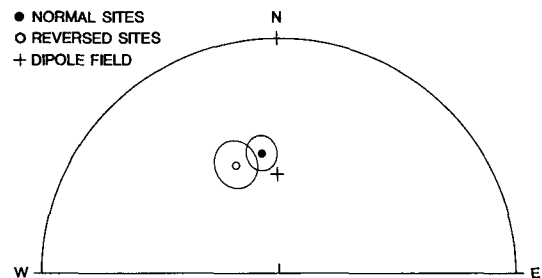


Figure 6. Reversals test for tilt-corrected data, showing statistically similar formational mean directions of normal and reversed populations, with the circles representing α_{95} confidence limits.

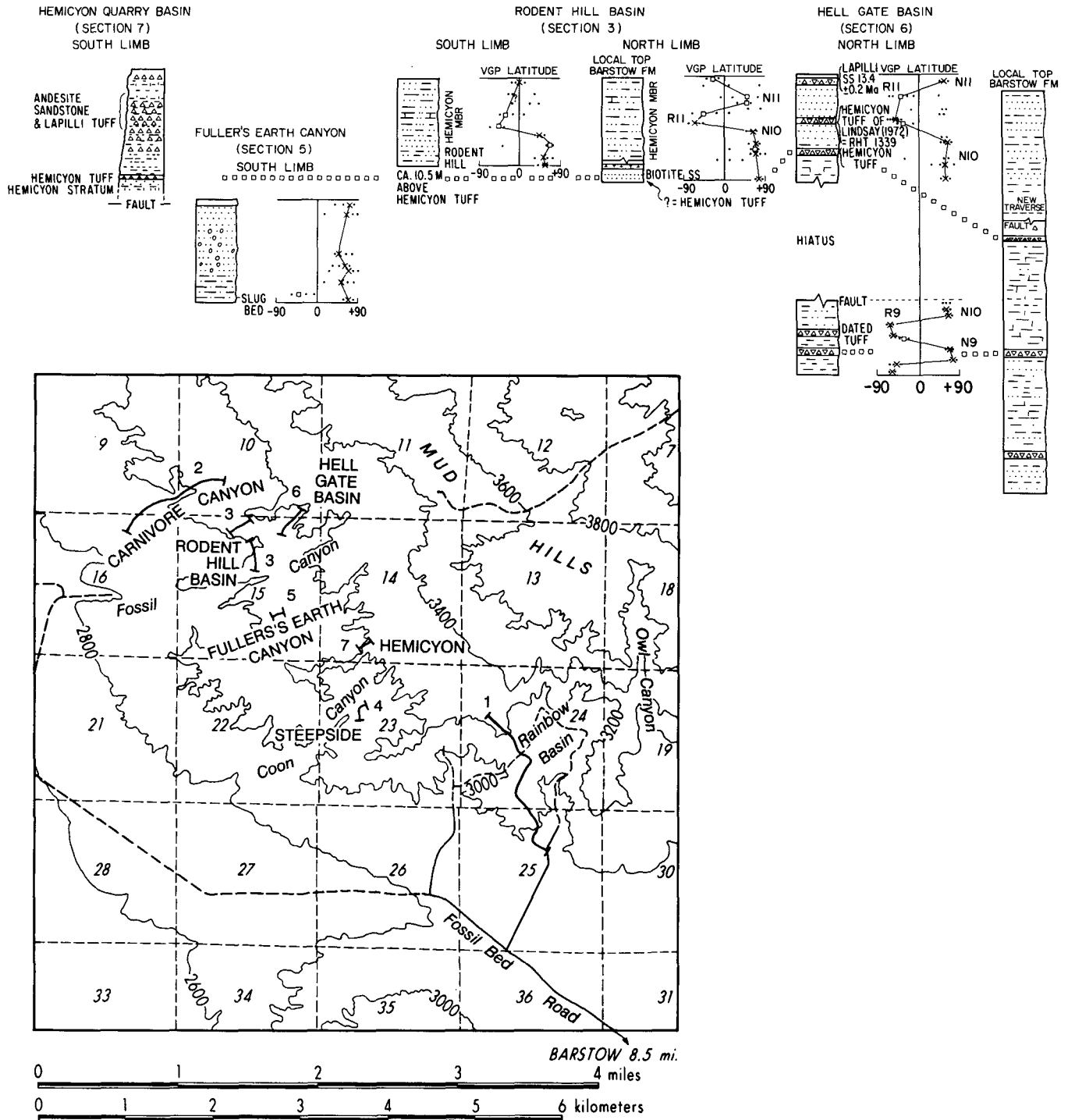


Figure 7. Lithostratigraphy, important marker horizons, magnetic polarity stratigraphy, and locations of our measured sections of the Barstow Formation in the Mud Hills. (Note overlap in center of measured sections.)

NEW ISOTOPIC DATES FROM THE BARSTOW FORMATION

In this section, we present new isotopic age determinations for the Barstow Formation in the Mud Hills, using ⁴⁰K-⁴⁰Ar (Table 2) and single-crystal laser-fusion ⁴⁰Ar/³⁹Ar (Table 3) techniques. Other relevant dates bearing on either regional correlations or calibration of the Barstovian

land-mammal age outside of California are presented in Woodburne and others (1990).

1. The Red Tuff

During the late stages of our field work, a new tuffaceous unit, herein termed the "Red Tuff," was discovered 15 m above the base of our

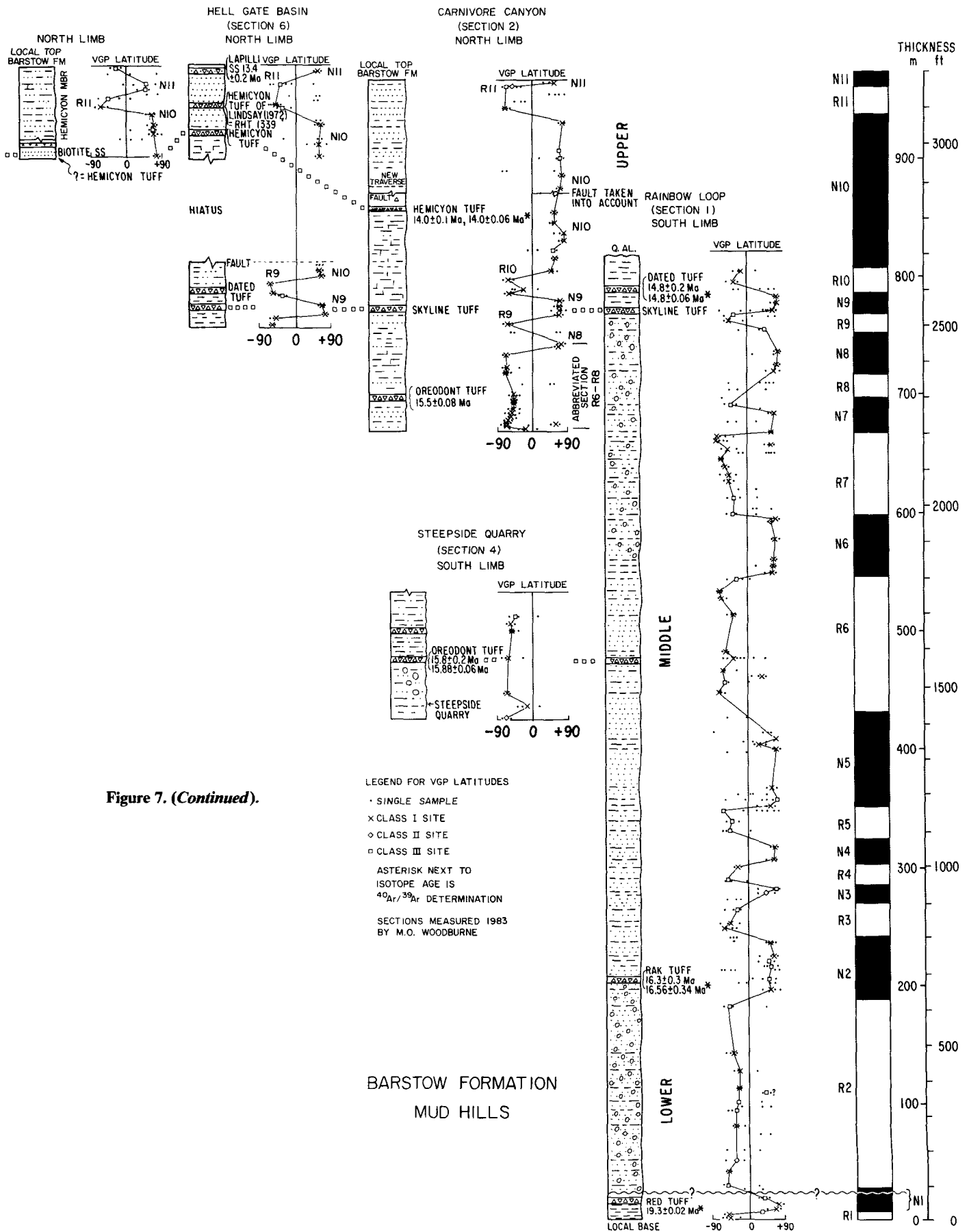


Figure 7. (Continued).

TABLE 2. ^{40}K - ^{40}Ar AGE DATA FOR THE BARSTOW FORMATION

Sample name	Sample number	KA number	Material dated	Weight (g)	% K mean	$^{40}\text{Ar}^*$ (mol/g)	% $^{40}\text{Ar}^*$	Age (m.y. \pm 1 σ)	Mean age [m.y. \pm σ (SEM)]	
Rak Tuff	86CS-BRB7	5336	Biotite	1.05443	5.289	$1.458 \cdot 10^{-10}$	21.8	15.84 ± 0.18	16.3 \pm 0.3 (0.2)	
		5336R	Biotite	0.73129	5.289	$1.506 \cdot 10^{-10}$	22.7	16.36 ± 0.19		
		5336R3	Biotite	0.20705	5.289	$1.514 \cdot 10^{-10}$	7.3	16.44 ± 1.1		
Oreodont Tuff	86CS-BCC1	5339R4	Sanidine	0.74256	8.548	$2.374 \cdot 10^{-10}$	66.8	15.95 ± 0.12	15.8 \pm 0.2 (0.17)	
		5339R5	Sanidine	0.68708	8.548	$2.325 \cdot 10^{-10}$	69.0	15.62 ± 0.12		
		5339R6	Sanidine	0.68708	8.548	$2.313 \cdot 10^{-10}$	63.8	15.53 ± 0.12		
	86CS-BCC1	5282	Biotite	1.02255	6.93	$1.743 \cdot 10^{-10}$	68.1	14.44 ± 0.12		
		5282R3	Biotite	0.70395	6.93	$1.774 \cdot 10^{-10}$	61.4	14.70 ± 0.14		
		CS8307	5404	Biotite	0.60615	7.283	$1.948 \cdot 10^{-10}$	78.0		15.36 ± 0.12
		5614	Biotite	0.70637	7.283	$1.970 \cdot 10^{-10}$	85.7	15.53 ± 0.12		
Dated Tuff	None	449R2	Biotite	1.05041	6.632	$1.700 \cdot 10^{-10}$	74.2	14.72 ± 0.13	14.8 \pm 0.1	
		RHT1348	70-12	Biotite	NA	5.93	$3.3478 \cdot 10^{-6}$	65.0		14.6
				Biotite	NA	5.93	$3.4354 \cdot 10^{-6}$	71.0		14.9
Hemicyon Tuff	RHT1343	70-13	Biotite	NA	5.92	$2.9075 \cdot 10^{-6}$	29.0	12.6	14.0 \pm 0.1 (0.05)	
			Biotite	NA	5.92	$3.2152 \cdot 10^{-6}$	43.0	14		
	CS8309	5403	Biotite	0.51235	6.613	$1.610 \cdot 10^{-10}$	59.7	13.99 ± 0.14		
		5403R	Biotite	0.4956	6.613	$1.620 \cdot 10^{-10}$	58.9	14.08 ± 0.25		
Lapilli Tuff	DES7017	2071	Biotite	0.8015	5.977	$1.409 \cdot 10^{-10}$	38.3	13.54 ± 0.14	13.4 \pm 0.2 (0.08)	
		2071R2	Biotite	0.70632	5.977	$1.378 \cdot 10^{-10}$	38.0	13.20 ± 0.14		
		2062	Plagioclase	2.5005	0.3431	$8.008 \cdot 10^{-12}$	19.6	13.41 ± 1.1		
		5501	Plagioclase	1.80263	0.3431	$8.086 \cdot 10^{-12}$	29.7	13.54 ± 0.47		

Decay constants: $\lambda_e + \lambda_g = 0.581 \times 10^{-10} \text{ yr}^{-1}$; $\lambda = 4.962 \times 10^{-10} \text{ yr}^{-1}$; $^{40}\text{K}/\text{K}_{\text{Total}} = 1.167 \times 10^{-4}$.

For calculation of (\pm) error, see discussion under methods in text.

KA 70-12 and 70-13 were analyzed by Teledyne Isotopes, contracted by R. H. Tedford (American Museum of Natural History). The ages were published by Woodburne and Tedford (1982); however, the analytical data were not included. The above data on these ages were made available by R. H. Tedford and are included here to clarify the origin of the 13.6 m.y. age published by these authors. Additional data are no longer available from Teledyne.

Note: KA 5339R6 is a second argon gas fraction of 5339R5 and does not represent a separate sample fusion. Although it shows the reproducibility of the same gas, only separate fusions are used in the calculation of the mean ages.

TABLE 3. $^{40}\text{Ar}/^{39}\text{Ar}$ AGE DATA FOR THE BARSTOW FORMATION

Sample number	Lab number	$^{40}\text{Ar}/^{39}\text{Ar}$	$^{37}\text{Ar}/^{39}\text{Ar}$	$^{36}\text{Ar}/^{39}\text{Ar}$	% ^{40}Ar	Age (m.y. \pm 1 σ)	Mean age [m.y. \pm 1 σ (SEM)]	
87CS-BRB8	857-06	3.99	0.05323	0.0016	87.9	19.32 ± 0.19	19.31 \pm 0.02 (0.01)	
87CS-BRB8	857-11	4.19	0.02605	0.0024	83.4	19.28 ± 0.42		
87CS-BRB8	857-14	4.36	0.06850	0.0029	80.5	19.34 ± 0.60		
86CS-RB7	234-16	20.37	0.01520	0.0587	14.7	14.99 ± 8.7	17.72 \pm 1.40 (0.41)	
86CS-RB7	234-03	19.51	0.02030	0.5490	16.8	16.40 ± 5.0		
86CS-RB7	234-18	21.00	0.09850	0.0597	16.0	16.75 ± 5.8		
86CS-RB7	234-01	20.90	0.01310	0.0592	16.2	16.92 ± 5.2		
86CS-RB7	234-11	18.45	ND	0.0508	18.5	17.05 ± 5.7		
86CS-RB7	234-05	23.02	0.03030	0.0661	15.1	17.40 ± 5.1		
86CS-RB7	234-10	14.68	ND	0.0372	25.0	18.34 ± 3.9		
86CS-RB7	234-14	21.19	0.04090	0.0592	17.4	18.39 ± 4.7		
86CS-RB7	234-13	18.71	0.04100	0.0506	20.1	18.77 ± 7.6		
86CS-RB7	234-12	23.17	0.09880	0.0656	16.3	18.89 ± 8.7		
86CS-RB7	234-19	13.97	ND	0.0334	29.3	20.41 ± 5.1		
86CS-BCC1	11-2	34.92	0.01340	0.0197	83.3	15.89 ± 0.18		15.88 \pm 0.06 (0.03)
86CS-BCC1	11-3	29.55	0.00069	0.0016	98.4	15.87 ± 0.28		
86CS-BCC1	11-4	30.76	0.01280	0.0052	95.0	15.95 ± 0.30		
86CS-BCC1	11-5	29.56	0.011	0.0001	98.7	15.93 ± 0.15		
86CS-BCC1	11-6	28.95	ND	0.0078	100.0	15.80 ± 0.15		
86CS-BRB4	283-10	3.21	0.165	0.00012	99.1	15.89 ± 0.50		
86CS-BRB4	283-11	3.19	0.468	0.00018	99.3	15.81 ± 0.66		
86CS-BRB4	283-12	3.26	0.148	0.00031	97.3	15.82 ± 0.70		
86CS-BRB4	283-13	3.18	0.171	0.00004	99.8	15.83 ± 0.50		
86CS-BRB4	283-14	3.32	0.501	0.00063	95.5	15.85 ± 0.65		
86CS-BRB4	283-14	3.17	0.244	0.00001	100.0	15.88 ± 0.50		
86CS-BCC1	232-2	3.92	0.0532	0.00357	73.0	14.31 ± 0.80	14.63 \pm 0.29 (0.13)	
86CS-BCC1	232-3	3.59	0.0314	0.00222	81.5	14.60 ± 0.60		
86CS-BCC1	232-4	4.04	0.0234	0.00388	71.4	14.40 ± 1.10		
86CS-BCC1	232-5	4.34	0.0328	0.00451	69.1	14.99 ± 0.87		
86CS-BCC1	232-6	4.55	0.0297	0.00531	65.4	14.85 ± 0.78		
KA 449	876-01	2.92	0.02807	0.0007	93.0	14.86 ± 0.28		14.81 \pm 0.06 (0.03)
	876-02	2.91	0.17257	0.0006	93.5	14.89 ± 0.46		
	876-03	3.41	0.02822	0.0024	78.9	14.71 ± 0.39		
	876-06	4.69	0.03825	0.0067	57.6	14.82 ± 0.29		
	876-07	3.01	0.04840	0.0011	89.8	14.79 ± 0.53		
	876-08	2.92	0.05043	0.0008	92.4	14.80 ± 0.31		
CS-8309	805-01	4.15	0.05102	0.0056	60.0	14.02 ± 0.47	14.00 \pm 0.09 (0.05)	
	805-02	4.97	0.04068	0.0086	49.0	13.70 ± 0.45		
	805-03	4.81	0.04419	0.0078	52.2	14.14 ± 0.48		
	805-04	4.81	0.02951	0.0070	54.6	13.95 ± 0.55		

ND: ^{37}Ar too low to be detected.

Decay constants: $\lambda_e + \lambda_g = 0.581 \times 10^{-10} \text{ yr}^{-1}$; $\lambda = 4.962 \times 10^{-10} \text{ yr}^{-1}$; $^{40}\text{K}/\text{K}_{\text{Total}} = 1.167 \times 10^{-4}$.

$^{40}\text{Ar}/^{39}\text{Ar}/\text{ArK} = 0.002$; $^{39}\text{Ar}/^{37}\text{Ar}/\text{ArCa} = 0.000730$; and $^{36}\text{Ar}/^{37}\text{Ar}/\text{ArCa} = 0.000277$.

measured section 1 and about 3 m below an unconformity or fault with the overlying continuous stratigraphic sequence. Three $^{40}\text{Ar}/^{39}\text{Ar}$ analyses on biotite yielded a mean isotopic age of 19.3 ± 0.02 m.y. (Table 3). These results are considered preliminary pending further stratigraphic and isotopic analyses of the lowermost part of the section.

2. The Rak Tuff

A volcanic sandstone 205 m above the base of our composite section (Fig. 7) occurs locally at the contact between the lower and middle parts of the Barstow Formation. This tuff, herein named the "Rak Tuff," is located on the south limb of the Barstow syncline west of the entrance to Rainbow Loop road in our Rainbow basin section (Fig. 7). Three separate ^{40}K - ^{40}Ar determinations on biotite yielded a mean age of 16.3 ± 0.3 m.y. for the Rak Tuff (Table 2). Some discussion is required here because the age of this tuff is somewhat ambiguous, and it is the only new date presented herein that does not coincide with the expected age extrapolated from the MPTS or when compared to other isotopic determinations.

The three ^{40}K - ^{40}Ar analyses on biotite separates yielded ages of 16.4 ± 0.19 (KA 5336R), 16.4 ± 1.1 (KA 5336R2), and 15.8 ± 0.18 m.y. (KA 5336; see Table 2). The biotite is somewhat altered and has a slightly oxidized appearance. This alteration is reflected by the low %K value of 5.3 (unaltered biotite is, in most cases, between 6%K and 7%K, Dalrymple and Lanphere, 1968).

With the hope of resolving the age of the Rak Tuff, some of the fresher looking, least altered grains were picked from the KA 5336 separate for $^{40}\text{Ar}/^{39}\text{Ar}$ laser-fusion analysis. Some of the grains were too small to yield sufficient amounts of gas for adequate ^{36}Ar measurement; however, 11 analyses yielded enough gas to measure ^{36}Ar above background values to be considered reliable. Two interpretations can be made from the data shown in Table 3. (1) The spread seen in the ages is a consequence of alteration resulting in differential loss of K and Ar, yielding younger and older ages than the geologic age of the biotite. The combined age for all of the analyses is 17.7 ± 1.4 m.y. (2) Alternatively, in addition to alteration, there is contamination from older biotite. Because the Rak Tuff is definitely reworked and contains abundant older rock fragments, this alternative is possible. Although only a small data set was obtained, a bimodal age could be interpreted with means of 16.56 ± 0.34 and 18.45 ± 0.42 m.y. An older age was not obtained on the bulk ^{40}K - ^{40}Ar analyses; however, the younger age of 16.56 ± 0.34 m.y. is close to the combined 16.3 ± 0.3 m.y. of the bulk analyses. Given the low percentage of radiogenic Ar and high analytical uncertainties obtained on these biotites, we prefer our ^{40}K - ^{40}Ar analyses of the Rak Tuff of 16.3 ± 0.3 m.y. We hope that further $^{40}\text{Ar}/^{39}\text{Ar}$ analyses will better refine the age of the Rak Tuff.

An age of 16.3 ± 0.3 m.y. for the Rak Tuff initially appeared inconsistent with the paleomagnetic signature (Fig. 7) and other isotopic dates. This young age could easily be attributed to the slightly altered state of the biotite. As discussed earlier, the %K content of the biotite is low (5.3%). A loss of K could result in a young age for the biotite; however, previous workers (Dalrymple and Lanphere, 1968) have shown that Ar and K are commonly lost at proportional rates during alteration, such that %K values ≥ 5 should yield reasonable ages. K values less than 5% have produced both older and younger numbers than the "true" geologic age of the given unit. If our interpretation of the data is correct, then the similarity in ages derived from the two types of isotopic analyses (Tables 2 and 3) may reinforce their credibility.

3. Oreodont Tuff

The stratigraphically next-highest unit that we dated is the Oreodont Tuff located near the middle of the Barstow Formation at 474 m and about 300 m below the Skyline Tuff (Fig. 7). A ^{40}K - ^{40}Ar mean age of 15.8 ± 0.2 m.y. from sanidine was obtained on two determinations from this unit (Table 2; the third determination reported there is not used because it is the second gas analysis of a single sample fusion). The Oreodont Tuff provides an important stratigraphic marker bed for the middle part of the Barstow Formation and has been traced by us from Coon Canyon to Carnivore Canyon and to the Rainbow Loop (Fig. 7). The dated sample was collected in Coon Canyon on the south limb of the Barstow syncline in our Steepslope Quarry section (Fig. 7). The tuff is stratigraphically just below the Oreodont Quarry, which has yielded early Barstovian fossils. Woodburne and Tedford (1982; also see Woodburne and others, 1990) reported a previous biotite ^{40}K - ^{40}Ar age of 16.3 ± 0.3 m.y. (average of three analyses) for the Oreodont Tuff. ^{40}K - ^{40}Ar analyses on biotites from the same sample yielded anomalously young ages of 14.4 and 14.7 m.y. (Table 2). A second sample of the Oreodont Tuff (CS8307) was collected in Carnivore Canyon and is a certain lateral equivalent of the lower part of our section 2. The biotite at this locality yielded a ^{40}K - ^{40}Ar date of 15.5 ± 0.08 Ma (Table 2), further corroborating the sanidine dates from the Steepslope Quarry section. The explanation for the anomalously young biotite ages derived from the Steepslope Quarry (Coon Canyon) section is not known. In addition, the sanidine from the Oreodont Tuff from Coon Canyon and a third locality in Rainbow basin was dated by the $^{40}\text{Ar}/^{39}\text{Ar}$ method. Five combined individual and multiple grain analyses of 86CS-BCC1 from Coon Canyon (Table 3) yielded an overall age of 15.9 ± 0.06 m.y. Six combined individual and multiple grain $^{40}\text{Ar}/^{39}\text{Ar}$ analyses of 86CS-BRB4 from Rainbow basin (Table 3) yielded a mean age of 15.85 ± 0.04 m.y. In summary, the close correspondence of the ages determined from the ^{40}K - ^{40}Ar and $^{40}\text{Ar}/^{39}\text{Ar}$ methods supports the accuracy of these results.

4. Dated Tuff

The Dated Tuff (see Sheppard and Gude, 1969; KA 449 of Evernden and others, 1964) occurs at 789 m in our Rainbow Loop measured section on the south limb (Fig. 7), about 17 m above the Skyline Tuff. The Dated Tuff is an important marker bed for the upper part of the Barstow Formation, and we report here a number of new age analyses of it. As noted above, Evernden and others (1964) reported a ^{40}K - ^{40}Ar biotite age of 15.5 m.y. (KA449) for this unit. Additional dates were made by Teledyne Isotopes in 1970 from a sample collected by R. H. Tedford (RHT1348, Table 2). This biotite separate was dated at 14.6 and 14.9 Ma (see Woodburne and Tedford, 1982; Woodburne and others, 1990). The original biotite separate dated by Evernden and others (1964) was available during this study. Examination of this biotite revealed devitrified glass and numerous oxidized biotite grains, both of which were removed from the sample. New K analyses resulted in a mean value of 6.9% as compared to 4.8% of Evernden and others (1964), and our radiogenic Ar analyses revealed 74% compared to 59%. A new calculated age of 14.7 ± 0.8 m.y. was obtained from the biotite separate from this tuff, which is in concordance with the age reported by Woodburne and Tedford (1982); however, the older age reported by Evernden and others (1964) is attributed primarily to the low %K value (also see discussion under Rak Tuff). The concor-

dance on the biotite ages from the two laboratories suggests a reliable and accurate age determination for this tuff. On the basis of 3 available ^{40}K - ^{40}Ar analyses (Table 2), an overall age of 14.8 ± 0.15 m.y. is suggested for the Dated Tuff of Rainbow basin. In addition, 6 $^{40}\text{Ar}/^{39}\text{Ar}$ analyses of the same biotite yielded a mean age of 14.8 ± 0.06 m.y. and therefore corroborate our ^{40}K - ^{40}Ar age.

5. Hemicyon Tuff

This tuffaceous unit, located at 845 m in section 2, provides an important marker bed for the upper part of the Barstow Formation. It should be noted that the exact stratigraphic height of the Hemicyon Tuff above the base of our composite section varies because of facies changes within the Mud Hills. Tedford (RHT 1343; Table 2, also see references cited above) collected a sample of this tuff on the north side of Fuller's Earth Canyon, Hell Gate basin, south limb of the Barstow syncline, which is equivalent to the 845 m level of our measured section 7 (Fig. 7) and about 90 m above the Skyline Tuff. A biotite separate (70-11) was dated by Teledyne Isotopes at 14.0 and 12.6 Ma (references cited above). On the basis of these determinations, Woodburne and Tedford (1982) published an averaged age for the Hemicyon Tuff of 13.3 ± 0.7 m.y. Of the two analyses, the first measured 43% radiogenic Ar for an age of 14.0 m.y., whereas the second yielded only 29%Ar with an age of 12.6 m.y. Due to the large discrepancy between these two analyses (that is, greater than 1σ error), averaging of just two determinations is of questionable validity. The first determination, yielding an age of 14.0 m.y., appears to be the more reliable, based on its higher percentage of radiogenic Ar and on concordance with both the ages of the stratigraphically higher Lapilli Sandstone and that of the underlying Dated Tuff of the Rainbow basin.

A new sample (CS8309) of the Hemicyon Tuff was collected during this study from Carnivore Canyon from our measured section 2 at the 845 m level (Fig. 7). Biotites were dated by the ^{40}K - ^{40}Ar method and yielded ages of 14.0 ± 0.26 (KA 5403) and 14.1 ± 0.36 m.y. (KA 5403R, Table 2). These ages are concordant with the previously reported 14.0 m.y. age on the Hemicyon Tuff (references cited above). We take the mean age for the Hemicyon Tuff as 14.0 ± 0.1 m.y. (Table 2). In addition, 4 $^{40}\text{Ar}/^{39}\text{Ar}$ age determinations on the same biotite yielded a mean age of 14.0 ± 0.09 m.y. (Table 3), and therefore corroborate our ^{40}K - ^{40}Ar age.

6. Lapilli Sandstone

Lindsay (1972, p. 8) published two ^{40}K - ^{40}Ar age determinations on biotite and plagioclase from the "Lapilli Sandstone" of 13.6 and 13.8 m.y., respectively. This unit is important because it constrains the age and helps to calibrate the correlation of the "busy" magnetic pattern at the top of our composite section. It occurs at 960 m and locally 30 m above the Hemicyon Tuff in our measured section 6 taken at Hell Gate basin (Fig. 7). New analyses of these separates during the present study yielded age determinations of 13.20 ± 0.14 m.y. (KA 2071R2) on biotite and 13.54 ± 0.47 m.y. (KA 5501) on plagioclase (Table 2). An overall age of the Lapilli Sandstone is taken here as 13.4 ± 0.2 m.y. (Table 2).

DISCUSSION AND SIGNIFICANCE

Correlation to the Magnetic Polarity Time Scale

As mentioned above, 170 (125 Class I, 4 Class II, and 41 Class III) of the originally sampled sites were used to interpret the magnetostratigraphy of the Barstow Formation. Given the pattern of magnetic polarity zones, the following isotopic age determinations were used to calibrate the corre-

lation (Fig. 8) to the Magnetic Polarity Time Scale (MPTS) of Berggren and others (1985). (1) The date of 16.3 ± 0.3 Ma (Rak Tuff), which lies within a predominantly normal magnetozone (N2), correlates to the middle of Chron C5C. This is corroborated by the presence of a relatively long reversed magnetozone (R2) directly below, which is correlated to C5C-R on the MPTS. (2) The date of 15.8 ± 0.2 Ma (Oreodont Tuff) lies within a relatively long reversed magnetozone (R6) in the local Barstow sequence. This zone correlates to C5B-R, which has an age range of 16.2 to 15.3 m.y. ago (Berggren and others, 1985). (3) The date of 14.8 ± 0.2 Ma (Dated Tuff) lies near a polarity boundary (magnetozone N9-R10) and in a mixed interval of the MPTS. A correlation to C5AD is generally consistent with the extrapolated age between 14.9 and 14.2 m.y. ago on the MPTS, although local magnetozone N9 is not recognized on the MPTS. (4) The dates of 14.0 ± 0.1 Ma for the Hemicyon Tuff and the local polarity signature (N10) most probably correlate to the bottom of C5AC. (5) The top of the Barstow Formation is constrained by a date of 13.4 ± 0.2 Ma for the Lapilli Tuff and is consistent with the extrapolated age of the R to N transition within C5AB of the MPTS at 13.5 m.y.

The generally good correspondence of the isotopic dates and paleomagnetic pattern of the lower 700 m of our composite section relative to the Berggren and others (1985) calibration suggests a unique first-order correlation to the MPTS. The middle Miocene, represented by the upper 300 m of the Barstow section, however, is magnetically very "busy." We realize that several subchrons within our section could have more than one correlation, given the error margins of the isotopic age constraints provided in this study. As a result of our correlation to the MPTS, the continuous part of the composite section of the Barstow Formation has a maximum age represented within the middle of C5D at 17.6 m.y. and a minimum age represented within C5AB at 13.5 m.y. Hemingfordian mammals are known to occur within the lower part of the Barstow Formation (Woodburne and others, 1990), and the overlying section has yielded typically Barstovian mammals. Our correlations to the time scale imply that the Hemingfordian-Barstovian boundary occurs within the bottom of the upper half of C5B, or about 16 Ma based on the fact that Steepside Quarry (section 4), with the earliest Barstovian mammals yet recognized in the Mud Hills (Woodburne and others, 1990), occurs about 30 m below the Oreodont Tuff which is dated at 15.8 ± 0.2 Ma.

Crustal Rotation and Tectonic Models for the Mojave Desert

Garfunkel (1974) presented a model in which right slip on the northwest-trending faults of the central Mojave Desert resulted from crustal accommodation of the left-lateral slip along the Garlock fault. As part of this process, the central Mojave Desert was considered to have been rotated counterclockwise by some 30° . Because that rotation possibly coincided with slip on the Garlock fault, it must have taken place during the past 5 m.y. and therefore should have affected pre-rotation rocks. Garfunkel stated (p. 1931): "the precise magnitude and timing of the rotation can be checked by paleomagnetic studies."

Kamerling and Luyendyk (1979), Luyendyk and others (1980), Hornafius and others (1986), and Carter and others (1987) suggested that a number of districts in southern California have undergone large-scale ($\sim 70^\circ$) clockwise rotation in the Miocene. This activity concluded about 5 Ma, when the modern ("inboard"; Atwater, 1970) strand of the San Andreas fault was established. The only Mojave Desert terranes proposed to have undergone clockwise rotation, however, are those bounded by east-west-trending faults, and so our data from the Barstow Formation have no direct bearing on their model. Recently, however, Carter and others (1987) suggested that regional counterclockwise rotation of about 15° has taken place in the Mojave Desert to accommodate about 100 km

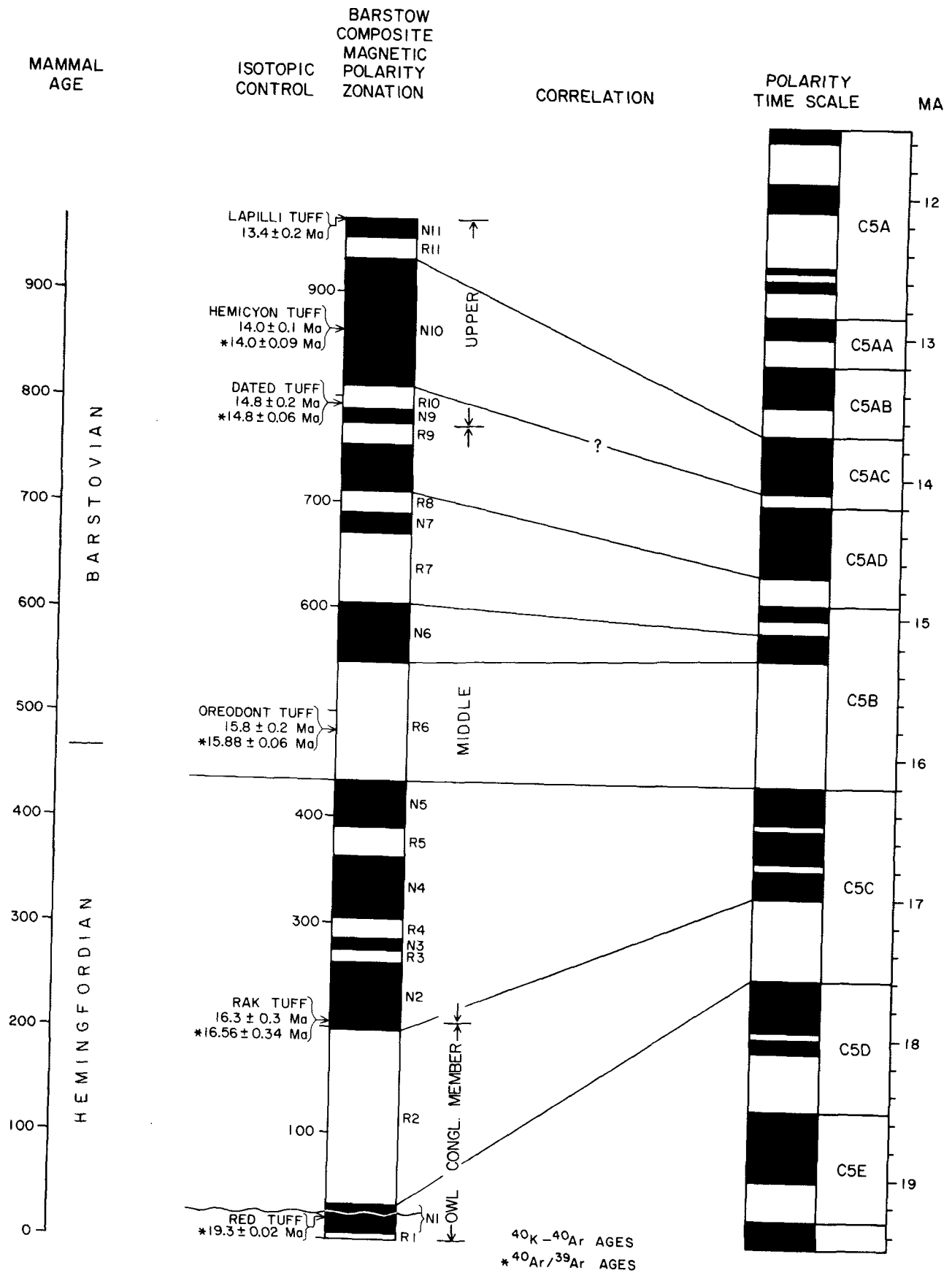


Figure 8. Correlation of the local composite magnetic polarity zonation of the Barstow Formation to the magnetic polarity time scale (Berggren and others, 1985).

of dextral shear across that area since the Miocene. Golombek and Brown (1988) studied the paleomagnetism of the 20 Ma Saddleback and Red Butte basalts from the northwestern Mojave Desert near Boron and Kramer Junction. Their data suggest $23.8^\circ \pm 11.3^\circ$ of clockwise rotation in that region since the extrusion of those rocks. More recently, Ross and others (1987, 1988, 1989) have suggested large clockwise rotations for several lower Miocene volcanic units in the central Mojave Desert. Also, Valentine and Brown (1987) determined that there was about 25° of counterclockwise rotation in the lower Miocene Pickhandle volcanic rocks, the unit that directly underlies the Barstow Formation in the central Mojave Desert.

Our data bear on the question of possible tectonic rotation of the Mojave block as represented from the paleomagnetism of the Barstow Formation (Table 1). If the formation mean of all sites (reversed inverted) is used, the declination of the Barstow Formation is $347.1^\circ \pm 7.97^\circ$ (Table 1, ΔD , declination error; Demarest, 1983; Beck and others, 1986). If the relevant North American pole of Irving (1979) is used, these results suggest slight counterclockwise, or if the ΔD is considered, negligible (that is, about 5° or less), rotation of the Barstow Formation since its deposition. If the late Oligocene-early Miocene reference pole for North America of Diehl and others (1983) is valid for middle Miocene rocks, then our data would suggest no rotation relative to the expected direction ($R = 4.1^\circ$; ΔR

$= 10.5^\circ$; rotation statistics from Demarest, 1983; Beck and others, 1986). Our results are confirmed by recent preliminary data from basalts in the Barstow Formation to the west of the Mud Hills where Valentine and others (1988) determined a mean declination of 342.6° ($\alpha_{95} = 23.5^\circ$), which overlaps our data set.

We also investigated whether any rotation occurred during the deposition of the Barstow Formation that might be masked by the formation mean. It appears that there is no trend in declinations observable throughout the composite section (Fig. 9). The negligible or slight counterclockwise rotation shown by our data from the Mud Hills suggests that this area was unaffected by rotations found in other studies within this region (references cited above) after deposition of the Barstow Formation between 19 and 13 Ma. Most of these studies, however, deal with earlier Miocene rocks. It is therefore possible that the principal rotations in much of the Mojave block are constrained to an interval during the early Miocene between 23 and 19 Ma.

It cannot be disputed that the tectonic history and degree of rotation of individual blocks in southern California is exceedingly complex. For the Mojave Desert, however, there seems to be a general pattern as follows (also see Ross and others, 1989; MacFadden and others, 1990). (1) Early Miocene (~ 20 m.y.) and older rocks demonstrate rotation, the exact amount and direction of which depends upon the local structural setting. (2) By about 19–13 Ma, that is, the time of deposition of the Barstow Formation, and thereafter, the central Mojave block is characterized by negligible or slight rotations (that is, 10° or less). This relative stability, however, is in marked contrast to the large amounts of rotation demonstrated to exist prior to the deposition of the Barstow Formation in the Mojave Desert and during the late Cenozoic elsewhere in southern California.

ACKNOWLEDGMENTS

This research was supported by National Science Foundation (NSF) Grant EAR82-06529. The isotopic age determinations were partially supported by NSF Grant EAR86-18701 to Garniss Curtis, Robert Drake, and Carl Swisher of the Berkeley Geochronology Center. Steven R. May of Exxon Research in Houston kindly gave us permission to use his data on the Barstow Formation, analyzed at the University of Arizona. Roy K. Dokka and Samuel Mukasa provided helpful comments that improved this study. We also thank D. E. Savage, G. H. Curtis, and R. H. Drake for their help in the field and laboratory.

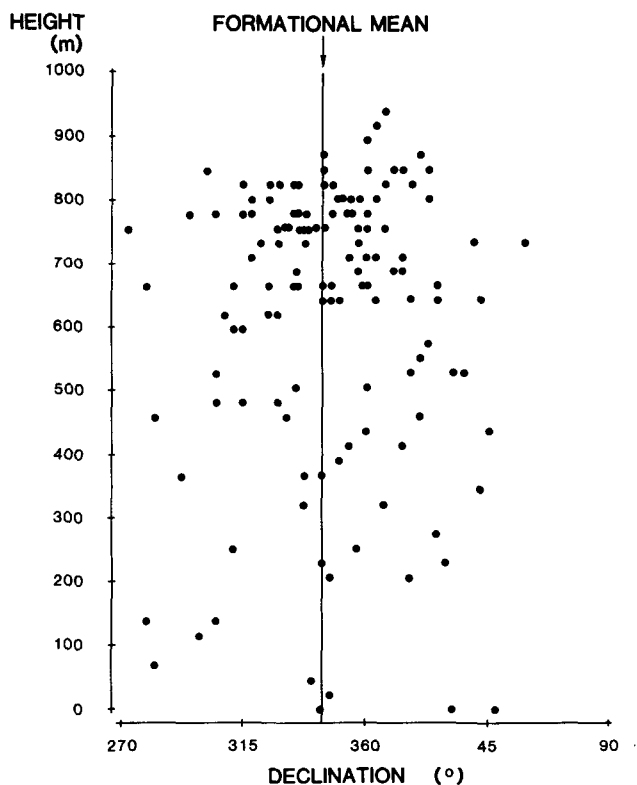


Figure 9. Plot of declination of all statistically significant site means from the Barstow Formation. Reversed site declinations were converted to northerly directions (by adding 180° to original value). Grand mean declination of the Barstow Formation is represented by vertical line.

REFERENCES CITED

- Atwater, Tanya, 1970, Implications of plate margins for the Cenozoic tectonic evolution of western North America: *Geological Society of America Bulletin*, v. 81, p. 3515–3535.
- Beck, M. E., Jr., Burmeister, R. F., Craig, D. E., Grommé, C. S., and Wells, R. E., 1986, Paleomagnetism of middle Tertiary volcanic rocks from the western Cascade series, northern California: *Journal of Geophysical Research*, v. 91, p. 8219–8230.
- Berggren, W. A., Kent, D. V., Flynn, J. J., and VanCouvering, J. A., 1985, Cenozoic geochronology: *Geological Society of America Bulletin*, v. 96, p. 3515–3535.
- Burke, D. B., Hillhouse, J. W., McKee, E. H., Miller, S. T., and Morton, J. L., 1982, Cenozoic rocks of the Barstow basin area of southern California—Stratigraphic relations, radiometric ages, and paleomagnetism: *U.S. Geological Survey Bulletin* 1529-E, p. 1–16.
- Carmichael, I.S.E., Hampe, J., and Jack, R. N., 1968, Analytical data on the U.S.G.S. standard rocks: *Chemical Geology*, v. 3, p. 59–64.
- Carter, J. N., Luyendyk, B. P., and Terres, R. R., 1987, Neogene clockwise tectonic rotation of the eastern Transverse Ranges, suggested by paleomagnetic vectors: *Geological Society of America Bulletin*, v. 98, p. 199–206.
- Dalrymple, B. G., 1979, Critical tables for conversion of K-Ar ages from old to new constants: *Geology*, v. 7, p. 558–560.
- Dalrymple, B. G., and Lanphere, M. A., 1968, Potassium-argon dating: San Francisco, California, W. H. Freeman, 258 p.
- Dalrymple, B. G., Alexander, E. C., Jr., Lanphere, M. A., and Kraker, G. P., 1981, Irradiation of samples for $^{40}\text{Ar}/^{39}\text{Ar}$ dating using the Geological Survey TRIGA reactor: *U.S. Geological Survey Professional Paper* 1176, 55 p.
- Demarest, H. H., Jr., 1983, Error and analysis for the determination of tectonic rotation from paleomagnetic data: *Journal of Geophysical Research*, v. 88, p. 4321–4328.

- Dibblee, T. W., 1968, Geology of the Fremont Peak and Opal Mountain quadrangles, California: California Division of Mines and Geology Bulletin, v. 188, 64 p.
- Diehl, J. F., Beck, M. E., Beske-Diehl, S., Jacobson, D., and Hearn, B. C., 1983, Paleomagnetism of the Late Cretaceous-early Tertiary north-central Montana alkalic province: *Journal of Geophysical Research*, v. 88, p. 10593-10610.
- Dokka, Roy K., 1983, Displacements on late Cenozoic strike-slip faults of the central Mojave Desert, California: *Geology*, v. 11, p. 305-308.
- , 1986, Patterns and modes of early Miocene crustal extension, central Mojave Desert, California: *Geological Society of America Special Paper* 208, p. 75-95.
- , 1988, Architecture of extensional domains of the Mojave rift: *Geological Society of America Abstracts with Programs, Cordilleran Section*, v. 20, p. 156.
- Dokka, R. K., and Woodburne, M. O., 1986, Mid-Tertiary extensional tectonics and sedimentation, central Mojave Desert, California: *Louisiana State University Publications in Geology and Geophysics, Tectonics and Sedimentation*, no. 1, 55 p.
- Evernden, J. F., Savage, D. E., Curtis, G. H., and James, G. T., 1964, Potassium-argon dates and the Cenozoic mammalian chronology of North America: *American Journal of Science*, v. 262, p. 145-198.
- Fisher, R. A., 1953, Dispersion on a sphere: *Royal Society of London Proceedings*, v. 217, p. 295-305.
- Fuller, M., Goree, W. S., and Goodman, W. L., 1985, An introduction to the use of SQUID magnetometers in biomagnetism, in Kirschvink, J. L., Jones, D. S., and MacFadden, B. J., eds., *Magnetite biomineralization and magnetoreception in organisms: A new biomagnetism*: New York, Plenum Press, p. 103-151.
- Garfunkel, Z., 1974, Model for the late Cenozoic tectonic history of the Mojave Desert, California, and for its relation to adjacent areas: *Geological Society of America Bulletin*, v. 85, p. 1931-1944.
- Golombek, M., and Brown, L., 1988, Clockwise rotation of the western Mojave Desert: *Geology*, v. 16, p. 126-130.
- Hornafius, S., Luyendyk, B. P., Terres, R. R., and Kamerling, M. J., 1986, Timing and extent of Neogene tectonic rotation in the western Transverse Ranges, California: *Geological Society of America Bulletin*, v. 97, p. 1476-1487.
- Irving, E., 1964, Paleomagnetism and its application to geological and geophysical problems: New York, John Wiley and Sons, 399 p.
- , 1979, Paleopoles and paleolatitudes of North America and speculations about displaced terrains: *Canadian Journal of Earth Sciences*, v. 16, p. 669-694.
- Johnson, N. M., and McGee, V. E., 1983, Magnetic polarity stratigraphy: Stochastic properties of data, sampling sets and the evaluation of interpretations: *Journal of Geophysical Research*, v. 88, p. 1213-1221.
- Kamerling, M. J., and Luyendyk, B. P., 1979, Tectonic rotations of the Santa Monica Mountains region, western Transverse Ranges, California, suggested by paleomagnetic vectors: *Geological Society of America Bulletin*, v. 90, p. 331-337.
- Kirschvink, J. L., 1980, The least-squares line and plane and the analysis of paleomagnetic data: *Royal Astronomical Society Geophysical Journal*, v. 62, p. 699-718.
- Lindsay, E. H., 1972, Small mammal fossils from the Barstow Formation, California: *University of California Publications in the Geological Sciences*, v. 43, p. 1-104.
- Luyendyk, B. P., and Hornafius, J. S., 1987, Neogene crustal rotations, fault slip, and basin development in southern California, in Ingersoll, R. V., and Ernst, W. G., eds., *Cenozoic basin development of coastal California (Rubey Volume 6)*: Englewood Cliffs, New Jersey, Prentice-Hall, p. 260-283.
- Luyendyk, B. P., Kamerling, M. J., and Terres, R., 1980, Geometric model for Neogene crustal rotations in southern California: *Geological Society of America Bulletin*, v. 91, p. 211-217.
- MacFadden, B. J., Woodburne, M. O., and Opdyke, N. D., 1990, Paleomagnetism and Neogene clockwise rotation of the northern Cady Mountains, Mojave Desert of southern California: *Journal of Geophysical Research* (in press).
- McElhinny, M. W., 1964, Statistical significance of the fold test in palaeomagnetism: *Royal Astronomical Society Geophysical Journal*, v. 8, p. 338-340.
- McFadden, P. L., and Jones, D. L., 1981, The fold test in palaeomagnetism: *Royal Astronomical Society Geophysical Journal*, v. 67, p. 53-58.
- Opdyke, N. D., Lindsay, E. H., Johnson, N. M., and Downs, T., 1977, The paleomagnetism and magnetic polarity stratigraphy of the mammal-bearing section of Anza-Borrego State Park, California: *Quaternary Research*, v. 7, p. 316-329.
- Rohlf, F. J., and Sokal, R. R., 1969, *Statistical tables*: San Francisco, California, W. H. Freeman, 253 p.
- Ross, T. M., Luyendyk, B., and Haston, R. B., 1987, Neogene tectonic rotations in the Cady Mountains, Mojave Desert, California: *Geological Society of America Abstracts with Programs*, v. 19, p. 824.
- , 1988, Paleomagnetic evidence for Neogene tectonic rotations in the central Mojave Desert, California: *Geological Society of America Abstracts with Programs, Cordilleran Section*, v. 20, no. 3, p. 226.
- , 1989, Paleomagnetic evidence for Neogene clockwise tectonic rotations in the central Mojave Desert, California: *Geology*, v. 17, p. 470-473.
- Sheppard, R. A., and Gude, A. J., III, 1969, Diagenesis of tuffs in the Barstow Formation, Mud Hills, San Bernardino County, California: *U.S. Geological Survey Professional Paper* 634, 35 p.
- Steiger, R. H., and Jaeger, E., 1977, Subcommittee on geochronology: Convention on the use of decay constants in geo- and cosmochronology: *Earth and Planetary Science Letters*, v. 36, p. 359-362.
- Tedford, R. H. (chairman), Skinner, M. F., Fields, R. W., Rensberger, J. M., Whistler, D. P., Galusha, T., Taylor, B. E., Macdonald, J. R., and Webb, S. D., 1987, Faunal succession and biochronology of the Arikarean through Hemphillian interval (late Oligocene through earliest Pliocene epochs) in North America, in Woodburne, M. O., ed., *Cenozoic mammals of North America*: Berkeley, California, University of California Press, p. 153-210.
- Valentine, M. J., and Brown, L., 1987, Tectonic rotation of the Barstow area, central Mojave Desert, California, inferred from paleomagnetic data: *EOS (American Geophysical Union Transactions)*, v. 68, p. 1254.
- Valentine, M. J., Brown, L., and Golombek, M., 1988, Counterclockwise Cenozoic rotations of the Mojave Desert: *Geological Society of America Abstracts with Programs, Cordilleran Section*, v. 20, no. 3, p. 239.
- Wood, H. E., II (chairman), Chaney, R. W., Clark, J., Colbert, E. H., Jepsen, G. L., Reeside, J. B., Jr., and Stock, C., 1941, Nomenclature and correlation of the North American continental Tertiary: *Geological Society of America Bulletin*, v. 52, p. 1-48.
- Woodburne, M. O., and Tedford, R. H., 1982, Litho- and biostratigraphy of the Barstow Formation, Mojave Desert, California, in *Geological excursions in the California desert*: Geological Society of America, Cordilleran Section, 78th Annual Meeting, Guidebook, p. 65-76.
- Woodburne, M. O., Tedford, R. H., and Miller, S. T., 1982, Stratigraphy and geochronology of Miocene strata in the central Mohave Desert, California, in *Geological excursions in the California desert*: Geological Society of America, Cordilleran Section, 78th Annual Meeting, Guidebook, p. 47-64.
- Woodburne, M. O., Tedford, R. H., and Swisher, C. C., III, 1990, Lithostratigraphy, biostratigraphy, and geochronology of the Barstow Formation, Mojave Desert, southern California: *Geological Society of America Bulletin*, v. 102, p. 457-475.

MANUSCRIPT RECEIVED BY THE SOCIETY JULY 27, 1988

REVISED MANUSCRIPT RECEIVED APRIL 20, 1989

MANUSCRIPT ACCEPTED JULY 18, 1989

UNIVERSITY OF FLORIDA CONTRIBUTION TO PALEOBIOLOGY NO. 315